Data-Driven Control of LVDC Network Converters: Active Load Stabilization

O.F. Ruiz-Martinez, J.C. Mayo-Maldonado, G. Escobar, B.A. Frias-Araya, J.E. Valdez-Resendiz, J.C. Rosas-Caro, P. Rapisarda

***Abstract*—This paper addresses the (model-free) data-driven control of power converters, acting as distributed generators, in low voltage direct current (LVDC) networks (e.g. DC microgrids, DC distributed power systems, DC buses wit multiple sources and loads, etc.). Since traditional stand-alone control design, cannot guarantee stability when converters are connected to a network, it is proposed a deterministic solution that does not require the network model– an approach purely based on measurement data. This is a suitable way to overcome common issues when using a model-based approach, e.g. the use of an excessive number of variables and equations, the presence of un-modeled dynamics, unknown parameters and/or the lack of first principle model equations. To corroborate the advantages of the proposed approach, the present work addresses an extreme but also realistic scenario: weak networks with active loads, such as constant power loads (CPLs). It is also shown that the proposed scheme guarantees stability in a rigorous deterministic way– using a Lyapunov approach based on coefficient matrices directly constructed from data. Simulation results using a multi-bus LVDC distribution network, based on PSCAD/EMTDC, are provided as proof of concept.**

***Index Terms*—Data-driven control, distributed generators, LVDC networks, DC microgrids, DC buses, oscillations, stability, constant power loads.**

I. Introduction

Switching converters are usually designed as *stand-alone* devices, i.e. they are closed-loop-tested using only nominal (resistive) loads. However, in practice their interconnection with other devices leads to unpredictable dynamical responses [1]. In a worst-case scenario, even though individually tested power converters exhibit a stable behavior, instability problems arise when used in DC networks, e.g., due to the *negative impedance* characteristics of regulated power devices, such as *constant power loads* (CPLs) (see [2]–[10]). To overcome this issue, we usually resort to a *model-based* paradigm: it is assumed that a model that represents the full DC network is always available to develop control strategies– in this way a stable optimal performance can be guaranteed.

Recent contributions of model-based approaches include: [11]–[13], where feedback control techniques are proposed to stabilize power converters in the presence of CPLs. In [2], [14]–[17], the design of controllers for simplified (cascade-converter) DC networks is introduced as a proof of concept. In [18]–[21], the concept of virtual impedance/admittance shaping is introduced as an intuitive way to mitigate the effect of negative impedance loads. Other contributions with similar aims, such as [22]–[24], induce a stabilizing damping component using feedback controllers.

These contributions are oriented to the modeling of the network, in particular in state-space form (i.e. using sets of first-order differential equations). This is not a sheer coincidence, since many compelling mathematical tools are available in such setting, for analysis and control design. However, *state models of networks are not a given* and their synthesis is not always an easy task. For instance, while the traditional state-space modeling is straightforward for individual power converters, this is not the case when there is an excessive number of variables and equations as in traditional networks, e.g., any device, component or even parasitic element with energy storage- or time-delay- characteristics, brings *at least* one additional variable and one differential equation. This modeling shortcoming is well-known in the context of smart grids, for which a paradigm-shift in the way we analyze and control the network is being required (see pp. 57-60 of [25]).

In order to solve the problem of unknown models, it is a common practice in control theory to perform system identification as a preamble of control design. See e.g. [26], where the known approaches require state-space- or (transfer function) port- variable data of the whole system. However, these approaches require an *a priori* defined restrictive mathematical structure to be *identified*, based on either state- or port- variable measurements, which unfortunately might be largely unavailable in practice. Consequently, although these settings have some compelling mathematical features, they are not able to address the modeling of the network in a general case– using a limited number of variables and sensors.

Motivated by these issues, this paper proposes a data-driven approach that is purely based on measurements, bypassing the need of mathematical models. Moreover, it is shown that this model-free approach can be completely deterministic, which is a mandatory characteristic to ensure stability and to display a robust performance.

Currently, there are a few deterministic contributions with similar goals, i.e., model-free with stability conditions. For instance, in [27] the authors propose a data-driven control for interlinked AC/DC microgrids based on input-output measurement data, using an adaptive observer. In [28], the control of a microgrid is proposed considering input-output data, that is

O.F. Ruiz-Martinez, J.C. Mayo-Maldonado (corresponding author, email jcmayo@tec.mx), G. Escobar, B.A. Frias-Araya and J.E. Valdez-Resendiz are with School of Engineering and Sciences at Tecnologico de Monterrey, Monterrey, Mexico.

J.C. Rosas-Caro is with Academia de Electrica, Electronica y Control at Universidad Panamericana, Zapopan, Mexico.

P. Rapisarda is with the Vision Learning and Control Group, University of Southampton, Great Britain.

used to construct a generic model for which a control design can be performed. In [29], a data-driven learning algorithm is used to identify a “local model network” that is controlled via “local linear controllers”.

These approaches provide plausible solutions that require in general, for practical purposes, a reasonable amount of recorded data to “train” or “tune” the controller. Unfortunately, they do not address the issue of stabilization, which is a required characteristic in the presence of active loads such as CPLs. As argued in this paper, this is in general a difficult problem, since stability margins are significantly shrunk when active loads such as CPLs are predominant. Consequently, it is necessary to endow controllers with additional stabilization capabilities. Since this task is difficult enough when using models, as shown in an extensive list of recent contributions, e.g. [2], [11]–[24], it is increasingly more challenging when full models are simply not available and controllers are set-up purely from data.

Prompted by these challenges, a new data-driven control approach for LVDC network converters is proposed. To do so, coefficient matrices constructed from data and an LMI-Lyapunov approach are used as efficient computational tools for control synthesis that guarantee stability, even when potentially unstable systems are treated. The proposed approach is illustrated by performing the control of a DC distributed generator connected to a network with CPLs. Regulation and stabilization features are also validated using simulations based on PSCAD/EMTDC.

II. Overview of the problem and summary of contributions

In this section, it is described in detail the problem of instability in LVDC networks due to CPLs, as well as the main features of the proposed contribution.

A. Problem formulation

The present work focuses on the fact that the nominal closed-loop performance of power converters is potentially degraded when tested over a network. This is due to the influence of other interconnected active loads, distributed generator dynamics and line impedances [1].

For instance, consider the dynamical equation of the output (capacitor) voltage in the traditional boost converter:

$$C\frac{d}{dt}v_o = (1-d)i_{in} - i_o; \tag{1}$$

where v_o, d, i_{in} and i_o are the output voltage, the duty cycle, the input- and the output- current, respectively. Consider the equilibrium of such equation, taking $\overline{v}_o$, $\overline{d}$, $\overline{i}_{in}$ and $\overline{i}_o$ as the corresponding steady-state quantities, i.e.

$$(1-\overline{d})\overline{i}_{in} = \overline{i}_o\ . \tag{2}$$

It is well-known that this equilibrium is satisfied in *stand-alone* operation– with a passive (resistive) load R demanding an output current $\overline{i}_o = \frac{\overline{v}_o}{R}$.

However, when the converter operates over a network, $\overline{d}$ is restricted to satisfy the desired DC bus voltage. Thus if i_{in} and i_o are independently manipulated, (2) cannot be automatically satisfied and the capacitor voltage cannot be constant– causing a detrimental uncoordinated performance by the interconnected converters. In a worst-case scenario, the resulting performance is even unstable, i.e. an equilibrium is never achieved (see e.g. the CPL problem in [2]–[6]).

To address this issue, this paper adopts the view of the network as a system whose behavior is determined by interconnected subsystems. Then, to perform a control design, we *zoom* into the network to focus on the converter to be controlled, which is interacting with the rest of the devices via electrical and control variables (e.g. voltages/currents and duty cycles). This is illustrated in Fig. 1.

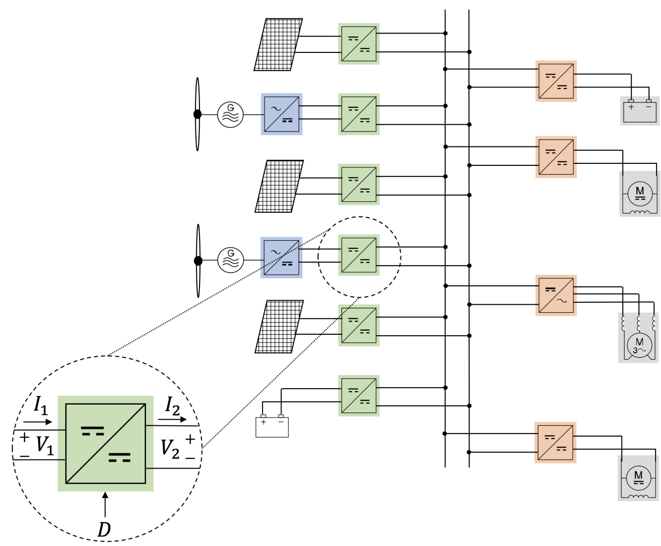

Fig. 1: Data-driven control of converters over networks by zooming.

The solution proposed in this paper is rested upon a suitable condition called *persistency of excitation*. This condition implies that measurement data can reveal the dynamics of all the devices that are influencing the behavior of the converter under study. This principle is used to (re-)design a controller from scratch– purely from experimental data– while ensuring a stable performance in a rigorous deterministic way.

B. Summary of advantages and contributions

In the following the main advantages and contributions of the proposed data-driven approach are outlined. These features are also described and justified in the detail along the paper.

1) Measurement data in limited quantities is sufficient for control purposes: Even though the largest possible amount of data would help to achieve maximum convergence, between the real network and the information gathered in data matrices; persistency of excitation does not specifically requires large amounts of data, but “sufficient” typical transients to recover the laws of the system. This is illustrated via small variations around the equilibrium that do not considerably deviate from the nominal operation of converters.

2) The least possible amount of sensors is required: Measurement of only the variables used for control, that satisfy in general standard observability/controllability properties, is required. Due to persistency of excitation, it is possible to recover the laws of the whole network without requiring full state- or port- variables in traditional state-space and transfer function approaches.

3) Stability is guaranteed in a rigorous deterministic way: Since this approach permits to recover the laws of the whole network from the measurement data, and DC-DC converters have only one equilibrium point (corresponding to the converter input/voltage gain equations), stability of such equilibrium is guaranteed using a Lyapunov LMI approach.

4) Stabilizability can be achieved: A significant distinctive component in our contribution is stabilizability, i.e. the control of an originally unstable system. This is a novel advantage that had not been yet explored in the existing literature of data driven-control for DC networks.

5) Gain tuning of commercial controllers or any desired linear control scheme can be used: To possibilities are open: 1) realization of a controller that can be even expressed in general higher-order shift operators (analogously higher order derivatives), for which state-space and transfer function are only special cases; and 2) realization of typical controller architectures that require only gain tuning to achieve stability– this option is of particular interest if a commercial device is restricting the controller configuration and only gain tuning can be performed.

6) Optimal control strategies and/or further performance specifications can be accommodated: Since the controller computation is set in terms of LMIs, it is possible to add further restrictions in the sense of optimal control, i.e. performance specifications in the form of linear matrix inequalities can be added. For instance, the LMI representation of functionals that enforce energy, time response, voltage/current variable relationships, etc..

The following section provides the theoretical elements that are instrumental for the development of the proposed data-driven control scheme, as well as the notation and concepts that are continuously used along this paper.

III. Preliminary background material

To make this paper self-contained, some preliminary material and notation is introduced. Further theoretical details in the context of control theory about *behavioral systems*, *quadratic difference forms* and *data-driven control*— that are used to develop the main results— can be found in [30], [31] and [32], respectively.

A. Notation

Consider $\mathbb{R}$, $\mathbb{Z}$ and $\mathbb{Z}_+$ the set of real, integer and positive integer numbers, respectively. The space of real vectors of dimension q is denoted by $\mathbb{R}^q$. The space of real matrices of dimension $p \times q$ is denoted by $\mathbb{R}^{p\times q}$. $\mathbb{R}^{\bullet\times\bullet}$ is used to denote real matrices with an unspecified number of rows and columns. I_q is the $q \times q$ identity matrix. Given two column vectors v_1 and v_2, $\mathrm{col}(v_1, v_2)$ is the vector obtained by stacking v_1 over v_2 in a single column vector. Given a matrix $A \in \mathbb{R}^{\bullet\times\bullet}$, $\mathrm{rank}(A)$ denotes its rank, while $\mathrm{vec}(A)$ denotes its column span, i.e., the set of all possible linear combinations of its column vectors. The *shift operator* σ applied to a function $f : \mathbb{Z}_+ \to \mathbb{R}^q$ is defined as $(\sigma f)(t) := f(t+1)$, which can be of order N, i.e., $(\sigma^N f)(t) := f(t+N)$ in general.

B. Linear difference systems

When dealing with sampled data, it is better to study dynamics in terms of discrete-time systems, using difference equations. Formally, a *linear difference system* can be expressed as

$$R_0 w + R_1(\sigma w) + \cdots + R_N(\sigma^N w) = 0, \tag{3}$$

where $w : \mathbb{Z}_+ \to \mathbb{R}^q$ is the function mapping discrete time points to the measured quantities, i.e., a finite time-series $w(1), w(2), ..., w(T)$; N is the maximum degree of the shift operator σ; and $R_i \in \mathbb{R}^{p\times q}$, with $i = 0, 1, ..., N$. Equation (3) can be represented compactly as

$$R(\sigma)w = 0; \tag{4}$$

which is called *kernel representation*; where $R(\sigma)$ is a polynomial matrix in σ, and represents a relationship among the set of measurements w in discrete time.

C. Quadratic difference forms

The stability properties of linear difference systems is studied by means of functionals. A *quadratic difference form* (QdF) is a functional of the discrete-time function w and its time-shifts, i.e.,

$$Q_K(w) = \begin{bmatrix} w^\top & \sigma w^\top & \cdots & \sigma^N w^\top \end{bmatrix} K \begin{bmatrix} w \\ \sigma w \\ \vdots \\ \sigma^N w \end{bmatrix}, \tag{5}$$

where K is called *coefficient matrix*. The *rate of change* ∇Q_K of a functional Q_K (which is analogous to a derivative in continuous-time) is defined as

$$\nabla Q_K(w)(t) := \sigma Q_K(w)(t) - Q_K(w)(t)\ . \tag{6}$$

D. Lyapunov stability

For analysis, a common definition for stability is used, i.e., a system represented by (3) is *asymptotically stable* if $\lim_{t\to\infty} w(t) = 0$ for all w that satisfies (3).

The well-known Lyapunov conditions (see, e.g., p. 2913 of [33]) are used to develop further algebraic specifications for stability, that will be instrumental for the synthesis of controllers. For ease of reference, these conditions are recalled as follows:

A system represented by (3) is asymptotically stable if there exist a QdF Q_K such that, for all w that satisfies (3), it holds that: 1) $Q_K \geq 0$; and 2) $\nabla Q_K < 0$. Moreover, the QdF Q_K satisfying the above inequalities is called *Lyapunov function* for (3).

Remark 1. Please notice that when dealing with higher order linear systems, it is only required a condition on the Lyapunov function Q_K to be non negative, rather than positive definite, please see [33]. □

IV. Suitability of data

Before introducing the main results, some important conditions are introduced to determine if the measured data are suitable for the analysis.

A. Data matrices

Since the scenario where the model of the DC network is unknown is considered, then sufficient conditions must be set to determine if the data contain enough information about its dynamics. To define such conditions, the concept of a matrix constructed from data is introduced.

Consider a time-series of length T expressed as $w(1), w(2), w(3), ..., w(T)$ that corresponds to a set of measurement data. A *Hankel matrix of depth* L, with $T > L \in \mathbb{Z}_+$ associated to this time-series is defined as

$$H_L(w) := \begin{bmatrix} w(1) & w(2) & \cdots & w\,(T-L+1) \\ w\,(2) & w\,(3) & \cdots & w\,(T-L+2) \\ \vdots & \vdots & \cdots & \vdots \\ w\,(L) & w\,(L+1) & \cdots & w\,(T) \end{bmatrix} . \quad (7)$$

Remark 2. It is expected that the length of the time-series denoted by T plays a role in the accurate management and quality of the data. For practical purposes, it will be taken “as long as possible” to ensure a better approximation to the “true system” (see [32]). The value of L will be relevant afterwards for properties that require rank verification and is associated to the maximum order of the shift operator of the system. □

B. Classification of variables

Given a set of network variables w, the type of available variables can be classified as either *input* or *output* variables. Input variables are independent (e.g. the duty cycle), while the output variables are consequences of the inputs (e.g. output-voltage). This concept is formalized next.

Given w that satisfies (3), the partition $w := \text{col}(u, y)$ is an *input/output partition* if

1) u is *free*, i.e., for all u there exists y such that $\text{col}(u, y)$ is an admissible trajectory of the system.
2) u is *maximally free*, i.e., given u, none of the components of y are free.
3) If 1) and 2) hold, then u is called an *input variable* and y an *output variable*.

In this paper control variables are used as inputs, i.e. duty cycles; while outputs are defined as the variables that serve to capture the influence of converter on the network, e.g. converter input/output voltages/currents.

C. Persistency of excitation

To specify mathematical conditions for the suitability of a set of data, the input variables are required to first satisfy the following condition: *A vector* $u = u(1), u(2), ..., u(T)$ *is persistently exciting of order* L *if* $H_L(u)$ *is of full row rank.*

Persistency of excitation has the following important implication according to [32]. Given a time-series

$$w = w(1), w(2), w(3), ..., w(T) =: \text{col}(u, y) \;, \quad (8)$$

that satisfies (3). If u is persistently excited of at least order L, where L is equal to the number of inputs and the dimension of the state-space (see Lemma 1 of [32]), then $\text{vec}(H_L(w))$ corresponds to the set of all possible solutions of (3).

In words, if the condition of persistency of excitation is satisfied, then the behavior of the network can be completely specified by the set of available measurements $w(1), ..., w(T)$. This means that any admissible trajectory of w can be recovered from such data.

Remark 3. In the stabilization case studied in this paper, the degraded unexpected dynamics of the converter when tested over a network are used. It is possible to take advantage from the fact that a controller that features robustness and stability only in stand-alone operation attempts to steer the voltage and current values to a desired equilibrium, but is in conflict with the dynamics of the constant power load– which produces an unstable (oscillating) performance. This actually facilitates the accomplishment of persistency of excitation condition– since the variations of the input are also persistent. On the other hand please notice that persistency of excitation is tested only using the input, that corresponds to the duty cycle of the converter and which can be freely manipulated as to satisfy such condition. However, measurements from an unstable performance are not a requirement, since many other trajectories can be also sufficiently informative– as long as the rank condition on $H_L(u)$ is satisfied. □

V. Data-driven control of LVDC network converters

In this section the main results about data-driven control of DC-DC converters over networks are introduced.

A. LMI condition for stability

A method to design stabilizing controllers from data is now introduces, based on the computation of standard *linear matrix inequalities* (LMIs). To do so, notice that the Lyapunov conditions 1)-2) recalled in Sec. III-D, are satisfied if there exists a QdF $Q_K \geq 0$ and polynomial matrices $Y(\sigma)$ and $F(\sigma)$ of suitable sizes such that

$$\begin{aligned}\sigma Q_K(w) - Q_K(w) + w^\top R(\sigma)^\top Y(\sigma) w + w^\top Y(\sigma)^\top R(\sigma) w \\ = -w^\top F(\sigma)^\top F(\sigma) w \;.\end{aligned} \quad (9)$$

Note that for every w that satisfies $R(\sigma)w = 0$, it follows that

$$\underbrace{\sigma Q_K(w) - Q_K(w)}_{=:\nabla Q_K} = -\|F(\sigma)w\|_2^2 \;; \quad (10)$$

which corresponds to a strictly negative rate of change. To develop a stability condition equivalent to (9) that can be easily tested and used for control design, note first that (3) can be written as

$$R(\sigma)w = \begin{bmatrix} R_0 & R_1 & \cdots & R_N \end{bmatrix} \begin{bmatrix} w \\ \sigma w \\ \vdots \\ \sigma^N w \end{bmatrix} . \quad (11)$$

The coefficient matrix is now defined as

$$\widetilde{R} := \begin{bmatrix} R_0 & R_1 & \cdots & R_N \end{bmatrix} . \tag{12}$$

Similarly, a coefficient matrix can be defined as

$$\widetilde{Y} := \begin{bmatrix} Y_0 & Y_1 & \cdots & Y_N \end{bmatrix} ; \tag{13}$$

for $Y(\sigma)$ in (9). Moreover, define

$$z^\top := \begin{bmatrix} w^\top & \sigma w^\top & \cdots & \sigma^N w^\top \end{bmatrix} . \tag{14}$$

Then, using these coefficient matrices as well as the definition of a QdF in (5), equation (9) can be expressed as

$$\begin{aligned} &\overbrace{z^\top \begin{bmatrix} 0_{q\times q} & 0_{q\times Nq} \\ 0_{Nq\times q} & K \end{bmatrix} z}^{\sigma Q_K(w)} - \overbrace{z^\top \begin{bmatrix} K & 0_{Nq\times q} \\ 0_{q\times Nq} & 0_{q\times q} \end{bmatrix} z}^{Q_K(w)} \\ &+ \quad \underbrace{z^\top \widetilde{R}^\top \widetilde{Y} z + z^\top \widetilde{Y}^\top \widetilde{R} z}_{w^\top R(\sigma)^\top Y(\sigma) w + w^\top Y(\sigma)^\top R(\sigma) w} \quad < 0 . \end{aligned} \tag{15}$$

where $K > 0$ has dimension $Nq \times Nq$ and the inequality "$<$" accounts for the negative element at the right hand side of (9). Then by standard linear algebra principles, such stability condition can be reduced to finding a matrix $K = K^\top > 0$, satisfying the following LMI:

$$\begin{bmatrix} 0_{q\times q} & 0_{q\times Nq} \\ 0_{Nq\times q} & K \end{bmatrix} - \begin{bmatrix} K & 0_{Nq\times q} \\ 0_{q\times Nq} & 0_{q\times q} \end{bmatrix} + \widetilde{R}^\top \widetilde{Y} + \widetilde{Y}^\top \widetilde{R} < 0 . \tag{16}$$

Notice that matrices K and $\widetilde{Y}$ can be numerically computed using standard LMI solvers such as `Yalmip`.

B. Computation of coefficient matrices from data

The *sufficiency of information* concept introduced in Section IV has two main consequences: 1) it defines a condition to test if the available data are suitable for control purposes; and 2) it provides a way to compute the left kernel of w, i.e., a set containing a polynomial matrix $R(\sigma)$ such that $R(\sigma)w = 0$. The second point can be formalized as follows.

Consider that $w = w(1), w(2), w(3), ..., w(T) =: \mathrm{col}(u, y)$ is a sufficiently informative time-series that satisfies (3). There exists $\widetilde{R} \in \mathbb{R}^{p\times(N+1)q}$ such that

$$\widetilde{R} \begin{bmatrix} w \\ \sigma w \\ \vdots \\ \sigma^N w \end{bmatrix} = 0 ; \tag{17}$$

for all w that satisfies (3).

In order to corroborate the validity of this statement and most importantly the computation of such matrix $\widetilde{R}$, it is shows that it is enough to apply *singular value decomposition* to the Hankel matrix, which is an easy matter for `MATLAB`.

Consider $H_{N+1}(w)$, where N corresponds to the maximum degree of the shift operator. Now consider the *singular-value decomposition (SVD)* of the Hankel matrix

$$H_{N+1}(w) := U \Sigma V^\top ; \tag{18}$$

where $U \in \mathbb{R}^{q\times q}$ and $V \in \mathbb{R}^{T\times T}$ are (square) orthogonal matrices; $\Sigma \in \mathbb{R}^{q\times T}$ is diagonal matrix with non-negative real numbers on the diagonal, and whose entries are called singular values. Moreover, there is an r number of non-zero singular values denoted by σ_i, $i = 1, ..., r$, for which $r := rank\,(H_{N+1}(w))$. Given a permanent regime measurement $w := \mathrm{col}(u, y)$ with an m number of inputs and an n number of outputs, $r = m$ corresponding to the linearly independent rows (the inputs). Note that

$$\begin{aligned} U^\top H_L(w) &= \Sigma V^\top , \\ &= \begin{bmatrix} \Sigma' & 0_{r\times(T-r)} \\ 0_{(q-r)\times r} & 0_{(q-r)\times(T-r)} \end{bmatrix} V^\top , \\ &= \begin{bmatrix} W \\ 0_{(q-r)\times(T-r)} \end{bmatrix} . \end{aligned} \tag{19}$$

where $\Sigma' \in \mathbb{R}^{r\times r}$ is a sub-diagonal matrix containing the non-zero singular values and W is a matrix of suitable size that represent the non-zero part of the product of $\Sigma V^\top$. It is concluded, from persistency of excitation and the last rows of zeros of such product, that $U^\top$ contains an annihilator of w, i.e. its left kernel, corresponding to its last $q - r$ rows. Consequently, consider the partition $U := \begin{bmatrix} U_1 & U_2 \end{bmatrix}$, where U_1 has r columns. Then, $\widetilde{R} := U_2^\top$ belongs to the left kernel of $H_{N+1}(w)$.

Matrix $\widetilde{R}$ contains sufficient information about the system from the gathered data. Following these results, the Algorithm in Fig. 2 is developed, which contains the computation of the coefficient matrix $\widetilde{R}$ from a set of measurement data.

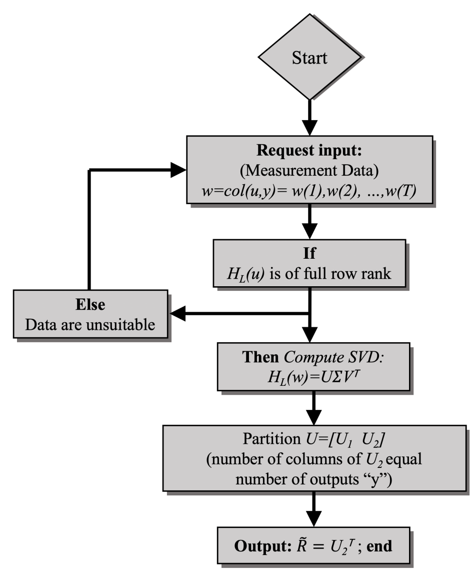

Fig. 2: Algorithm for the computation of the coefficient matrix $\widetilde{R}$ from measurement data.

The following section show how matrix $\widetilde{R}$ can be used for stabilizing control design.

C. Control design purely from data

This paper adopts a general point of view for control design in which a pre-defined controller structure (*P*, *PI*, *PID*, etc.) is not imposed. Instead, the proposed approach lets the available data itself to invoke the necessary mathematical restrictions for the plant to induce asymptotic stability for an originally unstable system. For ease of exposition and implementation, a state-space representation is used for the controller, though an even more general structure in higher-order terms is also permitted.

Let $w := \mathrm{col}(u, y)$ be the set of converter variables available for measurement. For practical purposes in a boost converter, the input $u := d$ is the duty-cycle, and the output $y := \mathrm{col}(i, v)$ comprises the input-current and output-voltage.

To facilitate the analysis, e.g., to study general stabilization properties at the origin, the "error" variables are used, which can be easily constructed from the data of measured variables and a desired steady state value (set-point), i.e.,

$$\hat{w} := w - \overline{w} \ ; \tag{20}$$

where $\overline{w}$ is the value of the measurement variables at a fixed, but otherwise arbitrary, admissible equilibrium. The following analogous notation for the input-output partition is used.

$$\hat{w} = \mathrm{col}(\hat{u}, \hat{y}) \ . \tag{21}$$

The unknown model of the converter interconnected to a DC-network is thus considered as being represented by

$$R(\sigma)\hat{w} = 0 \ ; \tag{22}$$

which can be congruently input-output partitioned as

$$\begin{bmatrix} R'(\sigma) & R''(\sigma) \end{bmatrix} \begin{bmatrix} \hat{u} \\ \hat{y} \end{bmatrix} = 0 \ ; \tag{23}$$

while the controller can adopt a general form

$$\sigma x' = Ax' + Bu' \ ; \quad y' = Cx' + Du' \ ; \tag{24}$$

where $x' : \mathbb{R} \to \mathbb{R}^n$, $A \in \mathbb{R}^{n\times n}$, $B \in \mathbb{R}^{n\times m}$, $C \in \mathbb{R}^{k\times n}$ and $D \in \mathbb{R}^{k\times m}$. A feedback controller can be established by considering as the measurement variables $\hat{w} = \mathrm{col}(\hat{u}, \hat{y})$ with definitions $y' := \hat{u}$ and $u' := \hat{y}$. This general form feedback controller with the realization (A, B, C, D) is depicted in Fig. 3.

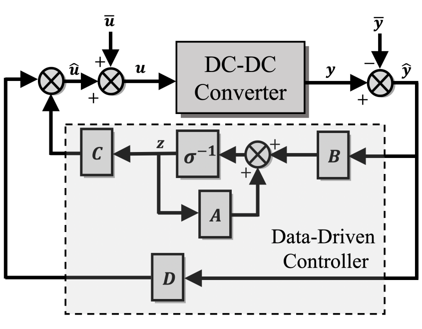

Fig. 3: General realization of a data-driven feedback controller in state-space form.

Note that this general family of controllers admits any P, PI, PID, state- and output- feedback configurations, among many other suitable possibilities. Consequently, in addition to the main motivation of bypassing the need of models for control design, it is also avoided the need to impose a particular controller architecture, since the data itself can determine the requirements for stabilization and set-point achievement.

This general converter-controller combination can thus be represented as

$$\underbrace{\begin{bmatrix} R'(\sigma) & R''(\sigma) & 0_{p\times q} & 0_{p\times k} & 0_{p\times n} \\ 0_{n\times k} & 0_{n\times m} & -B & 0_{n\times k} & \sigma I_n - A \\ 0_{m\times k} & 0_{m\times m} & -D & I_k & -C \\ -I_k & 0_{k\times m} & 0_{k\times q} & I_k & 0_{k\times n} \\ 0_{m\times k} & -I_m & I_m & 0_{m\times k} & 0_{m\times n} \end{bmatrix}}_{=:P(\sigma)} \begin{bmatrix} \hat{u} \\ \hat{y} \\ u' \\ y' \\ z \end{bmatrix} = 0 \ . \tag{25}$$

It is now possible to obtain the coefficient matrix $\widetilde{P}$ of $P(\sigma)$ as described in (11)-(12). Moreover, notice that coefficients $\widetilde{R}$ associated to $\begin{bmatrix} R'(\sigma) & R''(\sigma) \end{bmatrix}$ are directly obtained from the data and using Algorithm 1. Then A, B, C and D, which are now embedded in $\widetilde{P}$, can be computed using the augmented version of the stability condition in (16), i.e., an $Nr \times Nr$ matrix can be numerically found, with $r := q + k + m + n$, such that $K = K^\top > 0$ satisfies

$$\begin{bmatrix} 0_{r\times r} & 0_{r\times Nr} \\ 0_{Nr\times r} & K \end{bmatrix} - \begin{bmatrix} K & 0_{Nr\times r} \\ 0_{r\times Nr} & 0_{r\times r} \end{bmatrix} + \widetilde{P}^\top \widetilde{Y} + \widetilde{Y}^\top \widetilde{P} < 0 \ . \tag{26}$$

Remark 4. Since the parameters of both $\widetilde{P}$ and $\widetilde{Y}$ are unknown, condition (26) is, in general, a *bilinear matrix inequality (BMI)*, for which can be found by standard iterative algorithms (see e.g [34]). □

Remark 5. the fact that the controller computation is set in terms of LMIs, it is possible to add further restrictions in the sense of optimal control, i.e. performance specifications can be added in the form of linear matrix inequalities. For instance, the LMI representation of functionals that enforce energy, time response, voltage/current variable relationships, and so forth. The solution space of the controller gains is simply further restricted in order to satisfy performance specifications in a very straightforward way. For instance, given a functional $z^T Q z$ a condition to its coefficient matrix Q can be added to minimize its value, or to set limits with a simple additional inequality with $\epsilon > 0$, i.e.

$$Q - \widetilde{R}^\top \widetilde{Y} - \widetilde{Y}^\top \widetilde{R} \leq \epsilon I_{2(N+1)r}$$

in an analogous way as done for the stability condition. □

Remark 6. A general data-driven control perspective is provided, without resorting to "special structures". However, if in practice an implementation requires a very particular control structure, e.g., commercial devices where only gain modification is permitted. This problem can be addressed as a special case. Consider for instance a boost converter. The method uses error variables $\hat{w} := \mathrm{col}(\hat{d}, \hat{i}, \hat{v})$ that correspond to the duty cycle, the input-current and the output-voltage, respectively; and whose data can be experimentally obtained. Assume that its manufacture's predefined controller consists of the following equations:

$$\textit{Current loop:} \begin{cases} \hat{d} := -k_1 x - k_2 \hat{i} \ , \\ \sigma x = x + \hat{i} - i_{ref} \ ; \end{cases} \tag{27}$$

$$\textit{Voltage loop: } \begin{cases} i_{ref} := -\, g_1 z - g_2 \hat{v} \ , \\ \sigma z = z + \hat{v} \ ; \end{cases} \tag{28}$$

where $x, z : \mathbb{Z}_+ \to \mathbb{R}$ and k_i, g_i, $i = 1, 2$, are scalar quantities. Given this set of equations and considering the congruently partitioned unknown model of the DC network

$$\begin{bmatrix} R'(\sigma) & R''(\sigma) & R'''(\sigma) \end{bmatrix} \begin{bmatrix} \hat{d} \\ \hat{i} \\ \hat{v} \end{bmatrix} = 0 \ , \tag{29}$$

then the following augmented model can be constructed,

$$\underbrace{\begin{bmatrix} R'(\sigma) & R''(\sigma) & R'''(\sigma) & 0 & 0 \\ 1 & k_2 & 0 & k_1 & 0 \\ 0 & -1 & -g_2 & \sigma - 1 & -g_1 \\ 0 & 0 & -1 & 0 & \sigma - 1 \end{bmatrix}}_{=:P(\sigma)} \begin{bmatrix} \hat{d} \\ \hat{i} \\ \hat{v} \\ x \\ z \end{bmatrix} = 0 \ . \tag{30}$$

Then the computation of gains k_1, k_2, g_1 and g_2 can be numerically performed for this special case using (26). $\square$

VI. Comparison with state-of-the-art

In order to address a fair comparison between the contributions in this paper and the state-of-the-art, the main features of the proposed approach are illustrated with respect to [27], whose aims are the closest to ours. To show the differences between both methods MATLAB simulations of the closed-loop simulation of a single converter are provided, while in the following section the proposed approach will be extended for a full LVDC network using PSCAD/EMTDC. In this way it is possible to concentrate in illustrating the whole procedure, as well as the requirements, assumptions and limitations of both approaches.

A. Example for simulation

Consider a boost converter feeding a $5kW$ resistive load, which is later on changed into an active $5kW$ constant power load. The measurement of input-output data is considered, containing the input-current, output-voltage and the duty cycle, i.e. $y = \mathrm{col}(i, v)$ and $u = d$. With desired equilibrium of output voltage $\overline{v} = 380V$, input current $\overline{i} = 26.31$ and duty cycle $\overline{d} = 0.5$.

B. Theoretical principles behind each contribution

1) Contribution in [27]: is based on the implementation of the following observer-based discrete-time controller. Please note that the notation has been aligned with the one of the present paper to facilitate the exposition, i.e.

$$\begin{cases} \tilde{y}(k+1) = \tilde{y}(k) + \Phi(k)\hat{u}(k) + K(\tilde{y}(k) - y(k)) \\ \Phi(k+1) = \Phi(k) + (2\|\hat{u}(k)\|)\times \\ \qquad\qquad \Big(\tilde{y}(k+1) - \tilde{y}(k+1) - F\big(\tilde{y}(k) - y(k)\big)\Big)\hat{u}(k) \\ u(k) = u(k-1) + \Phi(k)^\top \left(\Lambda + \Phi(k)\Phi(k)^\top\right)^{-1} \times \\ \qquad\qquad \Big(\overline{y} - \tilde{y}(k) - K\big(\tilde{y}(k) - y(k)\big)\Big) \end{cases} ;$$

where y is the measured output; $\tilde{y}$ is the estimated output; $\hat{u} = u - \overline{u}$ is the incremental version of the input u with respect to its equilibrium value $\overline{u}$. Moreover, Φ is the estimated model of the system in a "pseudo-Jacobian" input-output form.

2) The present contribution: is based on the solution of a Lyapunov condition using matrices constructed from data, supported by the principle of persistency of excitation. In particular it is considered a time-series $w(1), w(2), w(3), ..., w(T)$. that corresponds to a set of measurement data. Then a *Hankel matrix* as in (7) is constructed. Then we perform the algorithm in Fig. 2 to obtain a matrix $\widetilde{R}$. As fully described in Sec. V-C, this matrix is used to construct $\widetilde{P}$, which contains the state-space matrices (A, B, C, D) of the controller. These matrices, now embedded in $\widetilde{P}$, are easily computed (e.g. using Yalmip) by solving the Lyapunov condition (26).

This method can be numerically performed in a recursive way if the plant is changed, to produce a new controller with guaranteed stability.

C. Requirements of data

1) Contribution in [27]: requires to satisfy general stability boundaries that can be previously set-up. Hence, theoretically speaking an equilibrium can be achieved from the beginning without data. Nevertheless a poor performance can be obtained, i.e. a desirable dynamic response cannot be specified without prior data. In order to fix this, it is highly recommended to use recorded data to "train" the controller. This is illustrated as follows.

For instance, as suggested by the Authors, we have set the following gains that satisfy stability conditions as in [27], i.e.

$$K := -0.8 \times I_2 \ ; \quad F := 10 I_2 \ ; \quad \Lambda := I_2 \ .$$

Then we obtain the traces shown in Fig. 4, which involves a poor dynamic response due to oscillations.

On the other hand, given recorded data, one can tune the gains of the estimator and controller to mitigate, e.g. oscillations and high overshoots. This action allows to obtain

$$K := -0.12 \times I_2 \ ; \quad F := 25 I_2 \ ; \quad \Lambda := I_2 \ .$$

The corresponding traces are shown in Fig. 5. Please notice that after tuning the parameters off-line, the estimation is improved as well as the whole closed-loop performance.

2) The present contribution: requires recorded data that satisfy persistency of excitation. This set of measurement data can be obtained either in open or closed loop operation (using any controller). In the given example we use very small variations on the duty cycle, between 0.47 and 0.53, during 0.02 seconds; Fig. 6. For simplicity, the example controller in Remark 6 is used. Then by performing the algorithm in Fig. 2 and solving the inequality (26), the following gains are obtained: $k_1 = 0.0002$; $k_2 = 0.0051$; $g_1 = 0.0025$; $g_2 = 0.0346$. The closed-loop traces are shown in Fig. 7.

D. Behavior when swapping resistances by active CPLs

As reported in the literature [2], [11]–[24], the inclusion of active loads such as CPLs is a very challenging scenario in

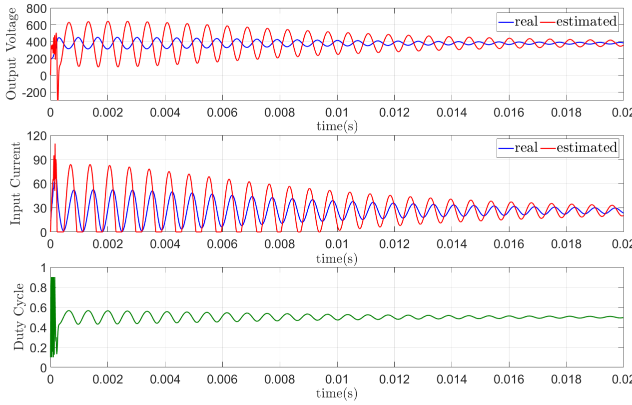

Fig. 4: Closed-loop response of the observer-based discrete-time controller.

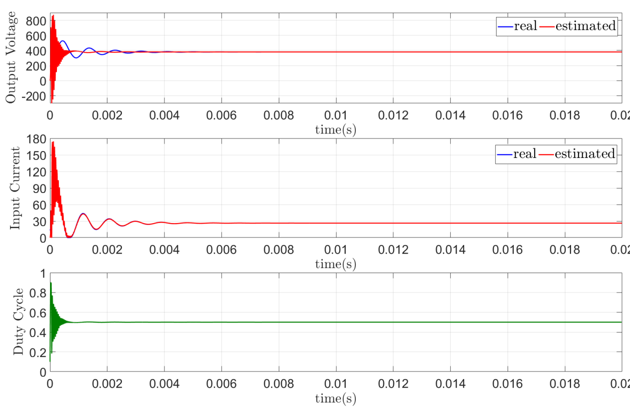

Fig. 5: Improved closed-loop response of the observer-based discrete-time controller after tuning when using prior data.

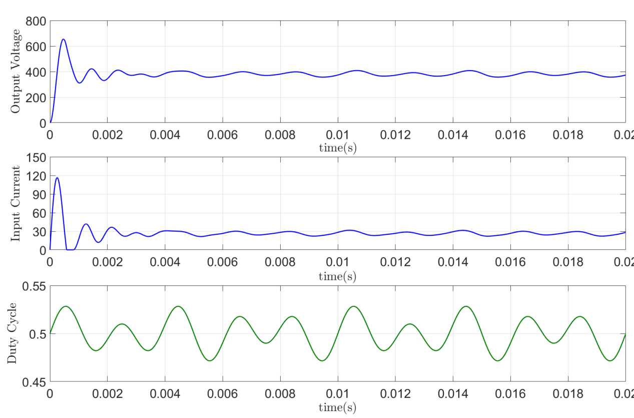

Fig. 6: Open-loop data for the data-driven controller.

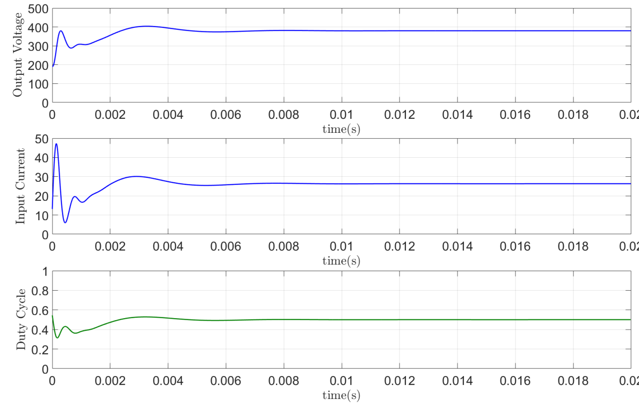

Fig. 7: Closed-loop response of the proposed data-driven controller.

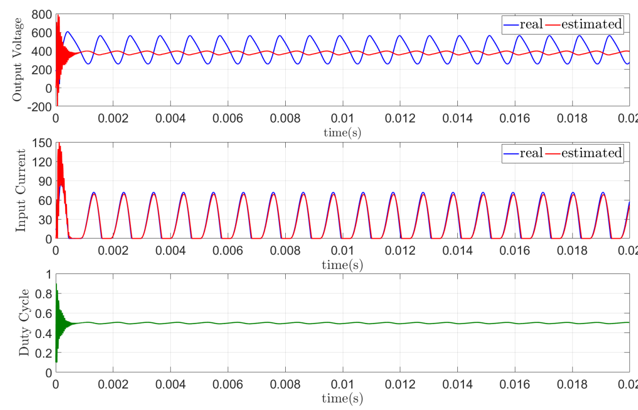

Fig. 8: Unstable performance of observer-based discrete-time controller when switching to an active load.

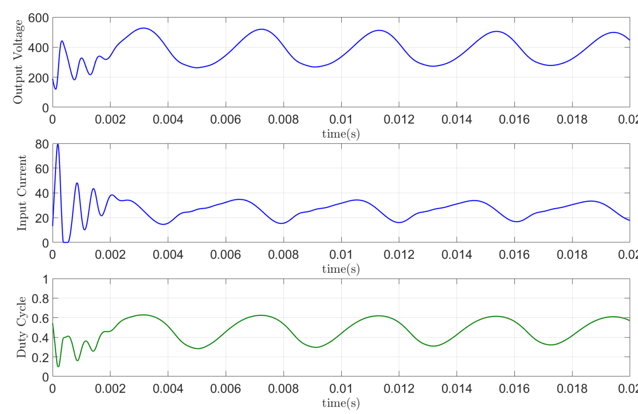

Fig. 9: Unstable performance when switching to an active load.

which originally stable controllers (set-up under pure resistive conditions) do not work in general. In this case, the controllers obtained in both approaches fall also into instability.

1) Contribution in [27]: falls into high amplitude oscillations as in Fig. 8.

2) The present contribution: also exhibits high amplitude oscillations when using the stand-alone computed gains. This is shown in Fig. 9. This situation can be easily overcome as detailed in the following section.

E. Main advantages of the present work

While up until now, both approaches ([27] and the present one) exhibit similar qualitative requirements, advantages and apparent limitations; the main advantage of the present approach is that it can overcome the instability issue if applied recursively. Hence, it is able to *stabilize*, i.e. it guarantees a stable equilibrium in systems that are originally unstable, due to the presence of active loads.

Although [27] contains a truly remarkable contribution, capable to control non-trivial interconnections, it is actually acknowledged by the Authors that boundedness in the original traces is required, which is parametrized by a Lipschitz condition (see the paragraph right before equation (4), on page 560 of [27]). Unfortunately, this is not possible when the converter exhibits high amplitude oscillations as reported by [2], [11]–[24] for LVDC networks; since such transients violate the Lipschitz condition. Take for example the current i induced by a load that demands constant power P, i.e.

$$i = \frac{P}{v} \; ;$$

this trajectory is neither globally, nor locally Lipschitz, since such condition must be satisfied for any arbitrary value of the voltage v, including the origin, for which the function is actually discontinuous.

On the other hand, since the present method can be applied recursively, it is enough to take e.g. the 0.02 seconds of an unstable transient as in Fig. 9, to use the same data to set-up new gains. By applying the algorithm in Fig. 2 and numerically solving (26), the following gains are obtained:

$$k_1 = 0.0033 \; ; \quad k_2 = 0.0095 \; ; \quad g_1 = 0.0046 \; ; \quad g_2 = 0.0628 \; .$$

Then the behavior in Fig. 10 is obtained. This result can be compared to all the previous traces that are evaluated up to $t = 0.02s$. In addition, in order to show that the new controller is highly robust, after 0.02 seconds, we abruptly increase and decrease the value of the active load from $5kW$ to $8kW$, then $3kW$ continuously, then it is observed that the controller compensates such variations by preserving stability.

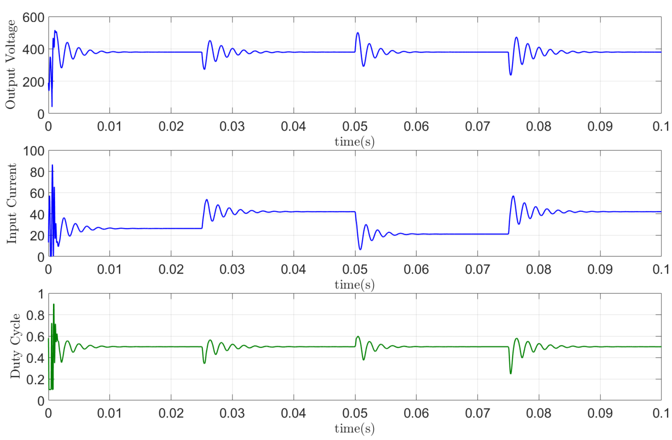

Fig. 10: Stabilization even under abrupt variations on the value of the active load: $5kW$ to $8kW$, then $3kW$ continuously.

The conclusion is that the present algorithm is able to guarantee stability when used recursively, even when switching to highly demanding and potentially unstable scenarios, i.e. to the case when active loads are predominant. The solution displays robustness against strong parametric changes. Moreover, only small quantities of data, either in open- or closed- loop are necessary to induce a rigorously guaranteed stable performance.

VII. Simulation results of a multi-bus LVDC network using PSCAD/EMTDC

In order to corroborate the advantages as well as the applicability of the proposed strategy, a series of simulations are performed based upon the network depicted in Fig. 11 which contains traditional passive and also active loads (CPLs), inducing a potentially unstable scenario. To facilitate the order of the simulations, each scenario is addressed in the following separated subsections. The parameters of the network are summarized in Table I and Table II.

The simulation was performed using the example controller in Remark 6, whose gains are computed using the data-driven scheme. A traditional droop control is used to define the reference for the DGs voltage as $v_{ref} = \overline{v} - K(i_o - \overline{i}_o)$ where are $\overline{v}$ and $\overline{i}_o$ are the nominal voltage and output current of the DG and i_o is the measurable output current of the DG. The gain was set up in a traditional way by defining the desired droop slope using

$$K = \frac{1}{5}\frac{\overline{v}}{\overline{i}_o} \; .$$

The solution rate for the discrete controllers is 100kHz, which is easily achieve in practice by standard (DSP/FPGA) micro-controllers.

A. Stand-alone (commercial) converter performance (nominal resistive load)

As a preamble of the main contribution, a controller that displays a good performance in terms of regulation and disturbance rejection for a DC-DC boost converter was implemented considering a nominal resistive load rated at $18kW$ at $380V$. A traditional linear controller as the one discussed in Remark 7 was used with the following gains:

$$k_1 := 0.0045 \; ; \quad k_2 := 0.0112 \; ; \quad g_1 := 0.0056 \; ; \quad g_2 := 0.0301 \; .$$

The closed-loop performance of the converter with a resistive, and under abrupt changes at the input-voltage is shown in Fig. 12. Notice that the performance is as expected by design, i.e., the response is asymptotically stable and the output-voltage is robustly regulated despite of the abrupt changes at the input-voltage. The purpose of this simulation is to show that even a robust controller can eventually become unstable in a network-connected scenario with CPLs.

B. LVDC network performance with interconnected converters and nominal resistive load

In this scenario, the converter with stand-alone dynamics reported in Fig. 12 is now connected to a LVDC network with only nominal resistive loads. The underlying converter is labelled as DG_1 and its dynamics as well as the rest of the other DG's (other converters') is reported in Fig. 13. It can be observed that the network displays a good performance as well as power sharing using the stand-alone controller design.

To show the robustness of the network under resistive load circumstances, a distributed generator (DG_5) is disconnected, then the power is redistributed among the other DGs and stability is preserved as illustrated in Fig. 14.

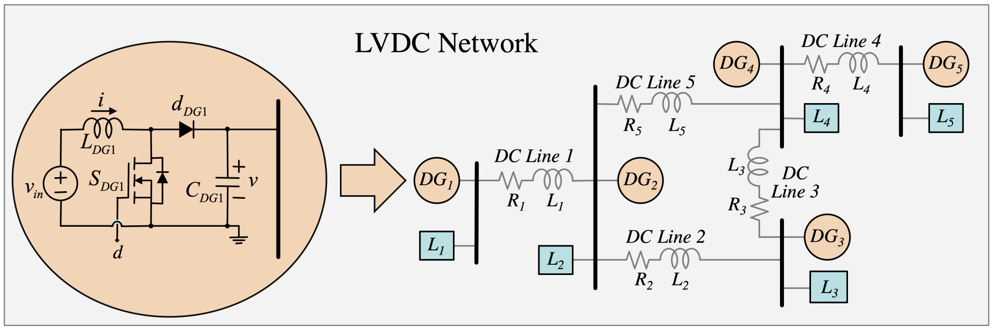

Fig. 11: LVDC network under study with potentially unstable dynamics due to CPLs.

TABLE I: Parameters of the simulation (DGs)

DG	*Gains* (k_1, k_2, g_1, g_2)	*Load*	V_{in}	V_{Bus}	*Type*	*Converter Parameters*
1	*(as specified in text)*	*18kW then 36kW (resistive +CPL)*	*200V*	*380V*	*boost*	$L = 250\mu H, C = 10\mu F$
2	*0.0028,0.0103,0.0025,0.231*	*16kW (resistive)*	*180V*	*380V*	*boost*	$L = 220\mu H, C = 15\mu F$
3	*0.0037,0.0099,0.0075,0.211*	*14kW (resistive)*	*160V*	*380V*	*boost*	$L = 210\mu H, C = 20\mu F$
4	*0.0043,0.0092,0.0033,0.108*	*12kW (resistive)*	*140V*	*380V*	*boost*	$L = 200\mu H, C = 10\mu F$
5	*0.0111,0.0136,0.0015,0.098*	*10kW (resistive)*	*120V*	*380V*	*boost*	$L = 220\mu H, C = 15\mu F$

TABLE II: Parameters of the simulation (DC lines)

DC Line 1	$0.05\Omega + 50\mu H$
DC Line 2	$0.02\Omega + 25\mu H$
DC Line 3	$0.02\Omega + 25\mu H$
DC Line 4	$0.02\Omega + 25\mu H$
DC Line 5	$0.05\Omega + 50\mu H$

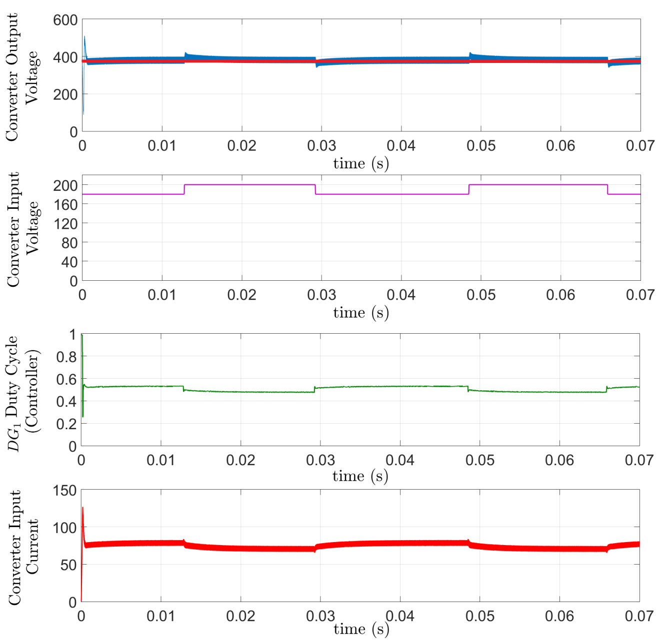

Fig. 12: Stand-alone (off-grid) performance of the converter under abrupt parametric changes.

C. LVDC network performance with interconnected converters and a constant power load.

In order to show the potential destabilizing effect of a active loads upon an originally stable network, it is now added in parallel to the resistive load in bus 1, a constant power load of $18kW$. The dynamic response of this action at the time $0.04s$ is shown in Fig. 15.

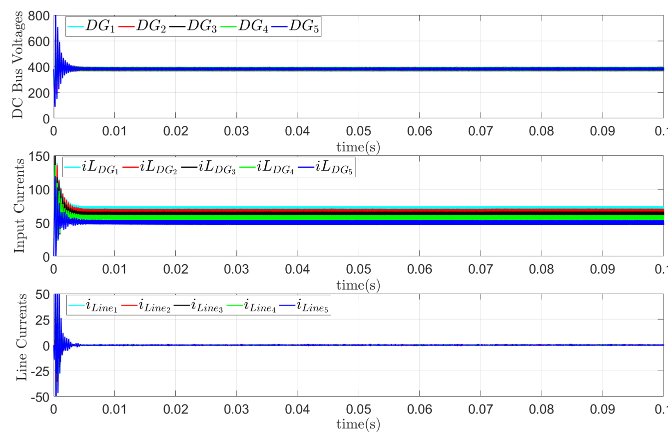

Fig. 13: Distributed generator voltages at each bus, their input current and the line currents between buses. Operation of stand-alone designed controller of DG_1 under pure resistive conditions.

The whole network displays an unstable, unacceptable behavior might prompt us to disconnect the DGs due to a highly degraded performance. However, in a matter of $0.1s$, one can even use the unstable dynamics to set-up the converter. Though it is important to emphasize that gathering data from unstable dynamics is an advantageous alternative rather than a requirement, since also stable or open-loop dynamics serve well to set-up the controller and guarantee stability in our approach. In order to set-up the controller, data of the duty cycle, DG voltage and input current of the DG_1 that is depicted in Fig. 16 is used. This simulation corroborates that limited data of $0.1s$ sampled at $100kHz$ is enough to synthesize the stabilizing controller.

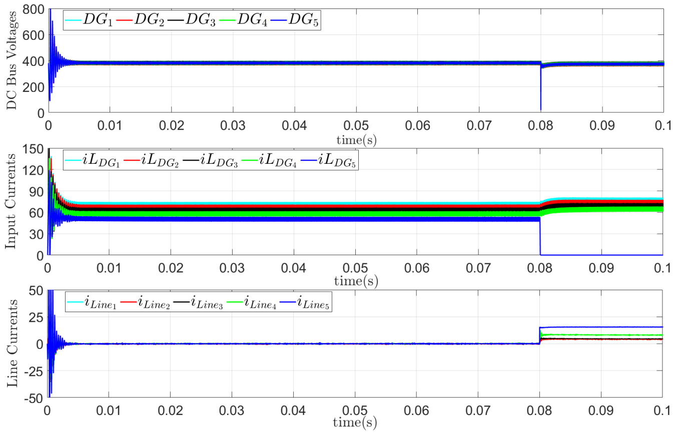

Fig. 14: Distributed generator voltages at each bus, their input current and the line currents between buses. Operation of stand-alone designed controller of DG_1 under pure resistive conditions when DG_5 is disconnected at $t = 0.08s$.

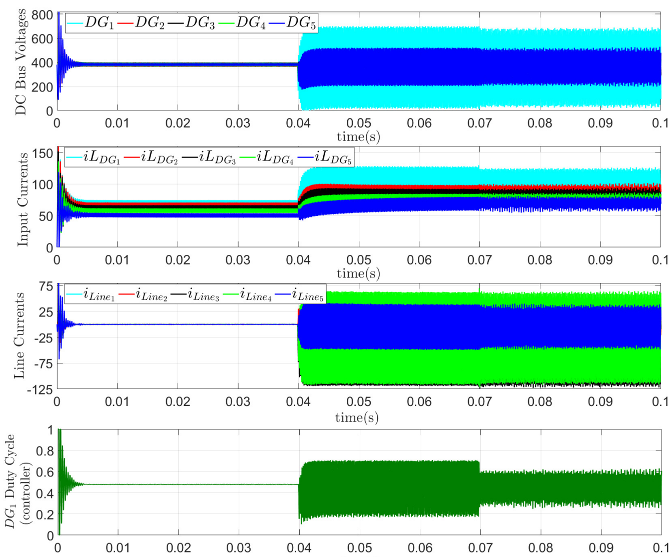

Fig. 15: Distributed generator voltages at each bus, their input current, the duty cycle (controller) and the line currents between buses. Operation of stand-alone designed controller when a new active constant power load of $18kW$ is added at bus 1 (demanding now $36kW$ at bus 1).

D. Stabilization of the LVDC network using the data driven controller.

Using the algorithm of Fig. 3 and by solving the LMI in (26), it is possible to reformulate the gains for DG_1, i.e.

$$k_1 := 0.0082\ ;\quad k_2 := 0.0429\ ;\quad g_1 := 0.0059\ ;\quad g_2 := 0.0853\ .$$

To show the effectiveness and stabilizing properties of the new controller, the same action of CPL interconnection performed in Fig. 15 is repeated. The simulation results are illustrated in Fig. 17.

It can be observed that the CPL destabilizing effect is now mitigated and the whole network exhibits an stable performance. Finally, to show the robustness of the proposed strategy, the same simulation performed as in the resistive case of Fig. 14 is repeated, this result is depicted in Fig. 18, where a robust stable performance is shown.

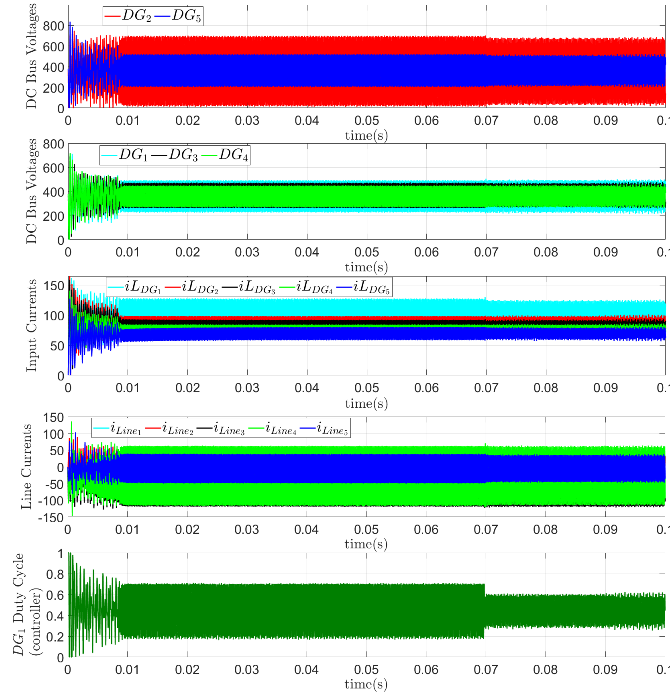

Fig. 16: Measurements under the CPL interconnection (only data for DG_1 is required, the rest of traces are included for illustrative purposes).

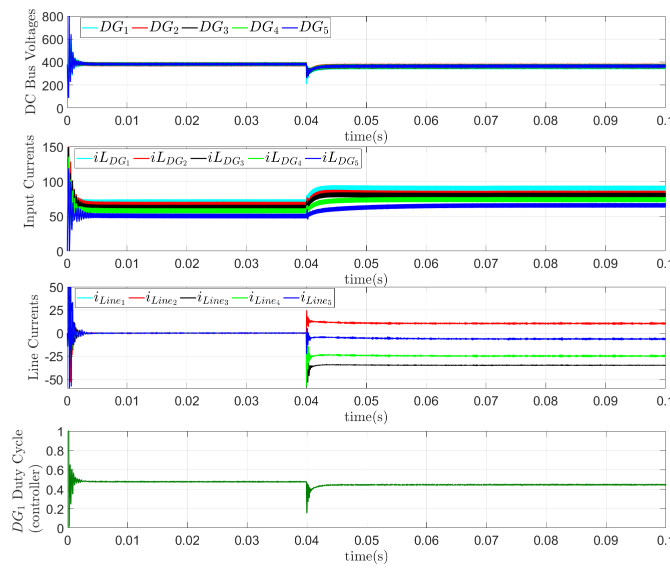

Fig. 17: Distributed generator voltages at each bus, their input current, the duty cycle (controller) and the line currents between buses. Operation of data-driven stabilizing controller when a new active constant power load of $18kW$ is added at bus 1 (demanding now $36kW$ at bus 1).

VIII. Conclusion

This work proposes a new data-driven approach to LVDC converter-network interconnections. The strength of this approach is its capability of stabilization of LVDC network converters in the presence of active loads. Moreover, the proposed scheme exhibits full flexibility: it does not require any information about the network model, and it does not assume any particular disturbance or instability mechanism. It is proposed to design controllers from scratch, by letting the data itself to invoke the necessary mathematical restric-

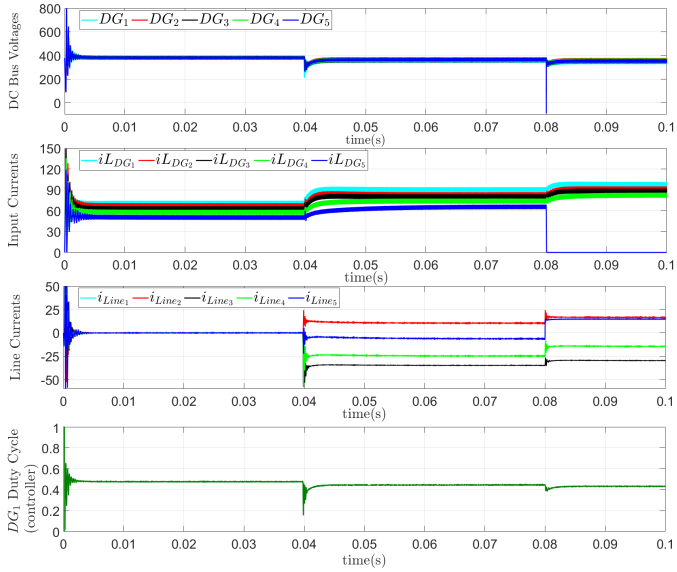

Fig. 18: Distributed generator voltages at each bus, their input current, the duty cycle (controller) and the line currents between buses. Operation of data-driven stabilizing controller when a new active constant power load of $18kW$ is added at bus 1 (demanding now $36kW$ at bus 1). Moreover, DG_5 is disconnected at $t = 0.08s$

tions required for stabilization– without imposing a particular structure. Moreover, special cases can be used if required, for example it is possible to rectify the misbehavior of a commercial controller by gain reformulation. Validation using PSCAD/EMTDC simulations in a realistic LVDC network conditions using CPLs was provided to corroborate the advantages of the proposed approach.

IX. Acknowledgements

The Authors wish to thank CONACyT and the Mexican Ministry of Energy (SENER) for their funding support under the project 266632, “Laboratorio Binacional para la Gestion Inteligente de la Sustentabilidad Energetica y la Formacion Tecnologica”.

References

[1] X. Feng, J. Liu, and F. Lee, “Impedance specifications for stable DC distributed power systems,” vol. 17, no. 2, pp. 157–162, Mar. 2002.
[2] Q. Xu, C. Zhang, C. Wen, and P. Wang, “A novel composite nonlinear controller for stabilization of constant power load in dc microgrid,” vol. 10, no. 1, pp. 752–761, Jan 2019.
[3] L. Herrera, W. Zhang, and J. Wang, “Stability analysis and controller design of dc microgrids with constant power loads,” vol. 8, no. 2, pp. 881–888, March 2017.
[4] M. Kabalan, P. Singh, and D. Niebur, “Large signal lyapunov-based stability studies in microgrids: A review,” vol. 8, no. 5, pp. 2287–2295, Sept 2017.
[5] H. Mosskull, “Optimal dc-link stabilization design,” vol. 62, no. 8, pp. 5031–5044, Aug 2015.
[6] T. Xisheng, D. Wei, and Q. Zhiping, “Investigation of the dynamic stability of microgrid,” vol. 29, no. 2, pp. 698–706, Mar. 2014.
[7] J. C. Mayo-Maldonado, J. E. Valdez-Resendiz, and J. C. Rosas-Caro, “Power balancing approach for modeling and stabilization of dc networks,” pp. 1–1, 2018.
[8] Z. Liu, M. Su, Y. Sun, H. Han, X. Hou, and J. M. Guerrero, “Stability analysis of dc microgrids with constant power load under distributed control methods,” vol. 90, pp. 62 – 72, 2018.
[9] C. Wang, J. Duan, B. Fan, Q. Yang, and W. Liu, “Decentralized high-performance control of dc microgrids,” vol. 10, no. 3, pp. 3355–3363, May 2019.
[10] J. Peng, B. Fan, J. Duan, Q. Yang, and W. Liu, “Adaptive decentralized output-constrained control of single-bus dc microgrids,” vol. 6, no. 2, pp. 424–432, March 2019.
[11] M. Su, Z. Liu, Y. Sun, H. Han, and X. Hou, “Stability analysis and stabilization methods of dc microgrid with multiple parallel-connected DC-DC converters loaded by cpls,” vol. 9, no. 1, pp. 132–142, Jan 2018.
[12] Y. Gu, W. Li, and X. He, “Passivity-based control of dc microgrid for self-disciplined stabilization,” vol. 30, no. 5, pp. 2623–2632, Sept 2015.
[13] M. K. Zadeh, R. Gavagsaz-Ghoachani, S. Pierfederici, B. Nahid-Mobarakeh, and M. Molinas, “Stability analysis and dynamic performance evaluation of a power electronics-based dc distribution system with active stabilizer,” vol. 4, no. 1, pp. 93–102, March 2016.
[14] J. Zeng, Z. Zhang, and W. Qiao, “An interconnection and damping assignment passivity-based controller for a DC-DC boost converter with a constant power load,” vol. 50, no. 4, pp. 2314–2322, July. 2014.
[15] Y. Huangfu, S. Pang, B. Nahid-Mobarakeh, L. Guo, A. K. Rathore, and F. Gao, “Stability analysis and active stabilization of on-board dc power converter system with input filter,” vol. 65, no. 1, pp. 790–799, Jan 2018.
[16] L. M. Saublet, R. Gavagsaz-Ghoachani, J. P. Martin, B. Nahid-Mobarakeh, and S. Pierfederici, “Asymptotic stability analysis of the limit cycle of a cascaded DC-DC converter using sampled discrete-time modeling,” vol. 63, no. 4, pp. 2477–2487, April 2016.
[17] L. Fangcheng, L. Jinjun, Z. Haodong, and X. Danhong, “Stability issues of $Z+Z$ type cascade system in hybrid energy storage system (HESS),” vol. 29, no. 11, pp. 5846–5859, Nov. 2014.
[18] B. H. Kim and S. K. Sul, “Shaping of pwm converter admittance for stabilizing local electric power systems,” vol. 4, no. 4, pp. 1452–1461, Dec 2016.
[19] A. Aldhaheri and A. H. Etemadi, “Stabilization and performance preservation of dc–dc cascaded systems by diminishing output impedance magnitude,” vol. 54, no. 2, pp. 1481–1489, March 2018.
[20] M. Hamzeh, M. Ghafouri, H. Karimi, K. Sheshyekani, and J. M. Guerrero, “Power oscillations damping in dc microgrids,” vol. 31, no. 3, pp. 970–980, Sept 2016.
[21] X. Lu, K. Sun, J. M. Guerrero, J. C. Vasquez, L. Huang, and J. Wang, “Stability enhancement based on virtual impedance for dc microgrids with constant power loads,” vol. 6, no. 6, pp. 2770–2783, Nov 2015.
[22] L. Guo, S. Zhang, X. Li, Y. W. Li, C. Wang, and Y. Feng, “Stability analysis and damping enhancement based on frequency-dependent virtual impedance for dc microgrids,” vol. 5, no. 1, pp. 338–350, March 2017.
[23] M. Zhang, Y. Li, F. Liu, L. Luo, Y. Cao, and M. Shahidehpour, “Voltage stability analysis and sliding-mode control method for rectifier in dc systems with constant power loads,” vol. 5, no. 4, pp. 1621–1630, Dec 2017.
[24] M. Wu and D. D. C. Lu, “A novel stabilization method of lc input filter with constant power loads without load performance compromise in dc microgrids,” vol. 62, no. 7, pp. 4552–4562, July 2015.
[25] Y. Xinghuo, C. Cecati, T. Dillon, and M. Simões, “The new frontier of smart grids,” vol. 5, no. 3, pp. 49–63, Sept. 2011.
[26] L. Ljung, *System identification*. Springer, 1998.
[27] H. Zhang, J. Zhou, Q. Sun, J. M. Guerrero, and D. Ma, “Data-driven control for interlinked ac/dc microgrids via model-free adaptive control and dual-droop control,” *IEEE Trans. on Smart Grid*, vol. 8, no. 2, pp. 557–571, March 2017.
[28] S. A. Hashjin and B. Nahid-Mobarakeh, “Active stabilization of a microgrid using model free adaptive control,” in *2017 IEEE Industry Applications Society Annual Meeting*, Oct 2017, pp. 1–8.
[29] K. Rouzbehi, A. Miranian, J. I. Candela, A. Luna, and P. Rodriguez, “Intelligent voltage control in a dc micro-grid containing pv generation and energy storage,” in *2014 IEEE PES T D Conference and Exposition*, April 2014, pp. 1–5.
[30] J. Polderman and J. Willems, *Introduction to Mathematical System Theory: A Behavioral Approach*. Springer, Berlin, 1997.
[31] O. Kaneko and T. Fujii, “Discrete-time average positivity and spectral factorization in a behavioral framework,” vol. 39, no. 1, pp. 31 – 44, 2000.
[32] T. Maupong and P. Rapisarda, “Data-driven control: A behavioral approach,” vol. 101, pp. 37–43, 2017.
[33] C. Kojima and K. Takaba, “A generalized lyapunov stability theorem for discrete-time systems based on quadratic difference forms,” in *Proceedings of the 44th IEEE Conference on Decision and Control*, Dec 2005, pp. 2911–2916.
[34] C. Papageorgiou and M. Smith, “Positive real synthesis using matrix inequalities for mechanical networks: application to vehicle suspension,” vol. 14, no. 3, pp. 423–435, May 2006.

Omar F. Ruiz-Martinez received the B.S. and M.Eng. degrees in electrical engineering from Instituto Tecnologico de Ciudad Madero, Mexico, in 2005 and 2010 respectively. He received a Ph.D. degree in Applied Sciences of Control and Dynamic Systems from the Instituto Potosino de Investigacion Cientifica y Tecnologica, San Luis Potosi, Mexico in 2017. He is currently a postdoctoral assistant at Tecnologico de Monterrey, Campus Monterrey, Mexico. He is member of the Sistema Nacional de Investigadores (level C) in Mexico. His research interests include applied control to power electronics converters, electronics systems design and energy conversion strategies.

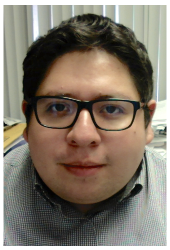

Jonathan C. Mayo-Maldonado received the B.S. and M.Eng. degrees in electrical engineering from Instituto Tecnológico de Ciudad Madero, Mexico, in 2008 and 2010 respectively. He received a Ph.D. degree in Electrical and Electronic Engineering from the University of Southampton, UK, in 2015. He was awarded with the Doctoral Control & Automation Dissertation Prize 2015 by the Institute of Engineering and Technology (IET), for his thesis entitled *Switched Linear Differential Systems*, supervised by Dr. Paolo Rapisarda. He is currently an Associate Professor at Tecnológico de Monterrey, Campus Monterrey, Mexico. He is member of the *Sistema Nacional de Investigadores (level 1)* in Mexico. His research interests include system and control theory, power electronics and smart grid technologies.

Gerardo Escobar received his PhD from the Signals and Systems Lab. LSS-SUPELEC, Université de Paris XI, France. From 2008 to 2012 he was a Principal Scientist in the Power Electronics Group at ABB Switzerland Ltd. He is currently a Professor-Researcher in the School of Engineering and Sciences at Tecnologico de Monterrey, Nuevo Leon, Mexico. He is Senior Member of the IEEE since 2008. He is member of the National Research Fellows System level 3 (SNI-3), CONACyT, Mexico. He served as AE of the IEEE Trans. on Industrial Electronics from 2007 to 2016. He is currently AE of the IEEE Trans. on Power Electronics since 2013. His main research interests include modeling, analysis, and control design of power electronic systems, and their applications in renewable energy systems, power quality, grid integration, active filters, inverters, DC-DC converters, multilevel converters, batteries, electrical drives, wind power, photovoltaic systems; as well as nonlinear control design, adaptive control, repetitive control, and their applications in current control, voltage balance, grid synchronization and harmonic compensation, among others.

Benjamin A. Frias-Araya received the Bachelor's Degree (Hons.) in Mechatronics Engineering from CETYS Universidad, Tijuana Campus, in 2016. In 2019, he received his Master of Science in Engineering (Hons.) from Tecnológico de Monterrey, Monterrey Campus. His research interests include electronics, power systems, control, mathematical modeling and data-driven theory.

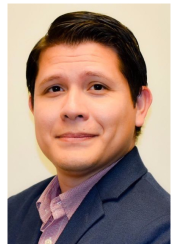

Jesus E. Valdez-Resendiz received the B.S. and M.Eng. degrees in electrical engineering from Instituto Tecnológico de Ciudad Madero, Mexico, in 2009 and 2011 respectively. He received a Ph.D. degree in Electronic Engineering from the Centro Nacional de Investigacion y Desarrollo Tecnologico, Mexico, in 2015. He is currently an Associate Professor at Tecnológico de Monterrey, Campus Monterrey, Mexico. He is member of the *Sistema Nacional de Investigadores* in Mexico. His research interests include power electronics, energy management, energy conversion and electric vehicles.

Julio C. Rosas-Caro received the B.S. degree in electronics and the M.S. degree in sciences in electrical engineering from the Instituto Tecnologico de Ciudad Madero, Mexico, in 2004 and 2005, respectively, and the Ph.D. degree in sciences in electrical engineering from the Cinvestav del IPN, Guadalajara, Mexico, in 2009. He has been a Visiting Scholar at the Michigan State University, University of Colorado Denver and the Ontario Tech. He is currently a Professor at Universidad Panamericana, Mexico. His research interest is power electronics including dc to dc converters, flexible alternating current transmission system devices, power converter topologies and applications.

Paolo Rapisarda took his Ph.D. working under the supervision of Jan C. Willems at the University of Groningen, The Netherlands. He is a full professor at the School for Electronics and Computer Science, University of Southampton, Great Britain. He is associate editor of the IEEE Transactions on Automatic Control, of Multidimensional Systems and Signal Processing, and of the IMA Journal of Mathematical Control and Information.